



This is a repository copy of *Analysis of s Duffing Oscillator that Exhibits Hysteresis with Varying Excitation Frequency and Ampitude.*

White Rose Research Online URL for this paper:  
<http://eprints.whiterose.ac.uk/85413/>

---

**Monograph:**

Li, L.M. and Billings, S.A. (2007) Analysis of s Duffing Oscillator that Exhibits Hysteresis with Varying Excitation Frequency and Ampitude. Research Report. ACSE Research Report 954 . Department of Automatic Control and Systems Engineering

---

**Reuse**

Unless indicated otherwise, fulltext items are protected by copyright with all rights reserved. The copyright exception in section 29 of the Copyright, Designs and Patents Act 1988 allows the making of a single copy solely for the purpose of non-commercial research or private study within the limits of fair dealing. The publisher or other rights-holder may allow further reproduction and re-use of this version - refer to the White Rose Research Online record for this item. Where records identify the publisher as the copyright holder, users can verify any specific terms of use on the publisher's website.

**Takedown**

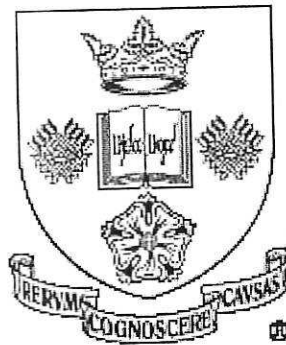
If you consider content in White Rose Research Online to be in breach of UK law, please notify us by emailing [eprints@whiterose.ac.uk](mailto:eprints@whiterose.ac.uk) including the URL of the record and the reason for the withdrawal request.



[eprints@whiterose.ac.uk](mailto:eprints@whiterose.ac.uk)  
<https://eprints.whiterose.ac.uk/>

# Analysis of a Duffing Oscillator that Exhibits Hysteresis with Varying Excitation Frequency and Amplitude

L.M.Li and S.A.Billings\*



Department of Automatic Control  
and Systems Engineering,  
University of Sheffield, Sheffield  
Post Box 600 S1 3JD  
UK

Research Report No. 954  
May 2007



## Analysis Of a Duffing Oscillator That Exhibits Hysteresis With Varying Excitation Frequency and Amplitude

L.M.Li and S.A.Billings\*

Department of Automatic Control and Systems Engineering  
University of Sheffield  
Sheffield S1 3JD  
UK

\*[S.Billings@sheffield.ac.uk](mailto:S.Billings@sheffield.ac.uk)

**Abstract:** Hysteresis, or jump phenomenon, are a common and severe nonlinear behaviour associated with the Duffing oscillator and the multi-valued properties of the response solution. Jump phenomenon can be induced by either varying the amplitude or the frequency of excitation. In this paper a new time and frequency domain analysis is applied to this class of system based on the response curve and the response spectrum map.

### 1. Introduction

Duffing's equation represents a class of single-degree-of-freedom nonlinear driven damped oscillators with a cubic, or more generally a polynomial, nonlinear restoring force, and has been widely used in modelling mechanical and electrical oscillators. Despite the seemingly simple form of Duffing's equation, it is extremely rich in dynamic behaviours and exhibits many complex solutions. Almost every nonlinear phenomenon can be found in Duffing's equation which has often been used as a benchmark example in many studies. Of the many complex nonlinear dynamics that are possible, a common severe nonlinear phenomenon that is induced by the multi-valued solution is due to the cubic nonlinearity in the Duffing oscillator is hysteresis, which is the topic of the current study.

Hysteresis can occur in the Duffing oscillator when either the amplitude or the frequency of the excitation is varied. Traditionally the 2-dimensional response curve, which displays the amplitude of response as a function of either the amplitude or the frequency of the excitation, has been used to study hysteresis (Stoker, 1950, Hagedorn, 1982 and Thompson and Stewart, 2002, etc). In this study, a new time and frequency domain analysis of hysteresis is presented. First a 3-dimensional response curve which takes account of both varying amplitude and frequency of the excitation



200568712



is introduced to provide a comprehensive view of hysteresis for a Duffing oscillator. Then a detailed qualitative analysis of various operating conditions along both excitation parameters is given, based on the response curves and response spectrum maps.

## 2. Volterra Series Representation of the Duffing Oscillator

The Volterra series, first proposed by Volterra (1930), has been widely used for the representation, analysis and design of nonlinear systems. The Volterra model is a direct generalisation of the linear convolution integral and provides an intuitive representation in a simple and easy to apply way. For a SISO nonlinear system, where  $u(t)$  and  $y(t)$  are the input and output respectively, the Volterra series can be expressed as

$$y(t) = \sum_{n=1}^{\infty} y_n(t) \quad (1.a)$$

and  $y_n(t)$  is the ' $n$ -th order output' of the system

$$y_n(t) = \int_{-\infty}^{\infty} \cdots \int_{-\infty}^{\infty} h_n(\tau_1, \dots, \tau_n) \prod_{i=1}^n u(t - \tau_i) d\tau_i \quad n > 0 \quad (1.b)$$

where  $h_n(\tau_1, \dots, \tau_n)$  is called the ' $n$ th-order kernel' or ' $n$ th-order impulse response function'. If  $n=1$ , this reduces to the familiar linear convolution integral.

The discrete time domain counterpart of the continuous time domain SISO Volterra expression (1) is

$$y(k) = \sum_{n=1}^{\infty} y_n(k) \quad (2.a)$$

where

$$y_n(k) = \sum_{-\infty}^{\infty} \cdots \sum_{-\infty}^{\infty} h_n(\tau_1, \dots, \tau_n) \prod_{i=1}^n u(k - \tau_i) \quad n > 0, k \in \mathbb{Z} \quad (2.b)$$

In practice only the first few kernels are studied on the assumption that the contribution of the higher order kernels falls off rapidly. Systems that can be adequately represented by a Volterra series with just a few terms are called weakly or mildly nonlinear systems. A discrete time Volterra series is also called a NX (Nonlinear model with eXogenous inputs) model.

The multi-dimensional Fourier transform of  $h_n(\cdot)$  yields the ' $n$ th-order frequency response function' or the Generalised Frequency Response Function (GFRF):

$$H_n(\omega_1, \dots, \omega_n) = \int_{-\infty}^{\infty} \cdots \int_{-\infty}^{\infty} h_n(\tau_1, \dots, \tau_n) \exp(-j(\omega_1 \tau_1 + \dots + \omega_n \tau_n)) d\tau_1 \cdots d\tau_n \quad (3)$$

The generalised frequency response functions represent an inherent and invariant property of the underlying system, and have proved to be an important analysis and design tool for characterising nonlinear phenomena. Despite its importance, the Volterra series has a limited convergence, and can therefore only be applied to so-called weakly or mildly nonlinear systems.

Consider a Duffing oscillator, with cubic nonlinearity, subject to a sinusoidal excitation as

$$m\ddot{y} + cy + k_1y + k_3y^3 = u \quad (4)$$

where  $u = A \cos(\omega t)$  and  $m, c, k_1$  and  $k_3$  are the mass, the damping, the linear stiffness and nonlinear stiffness respectively. The nonlinear stiffness parameter  $k_3$  in (4) needs to stay small in order to be 'weakly' nonlinear, at least in some regions, for the existence of Volterra series representation. When hysteresis, which is seen as a part of the class of 'severely' nonlinear phenomenon, occurs in the Duffing oscillator, a valid and unique global Volterra series representation would not be expected to exist. However, Duffing's oscillator with hysteresis may accept a local Volterra series representations. This point will be discussed in the following sections.

### 3. A 3-Dimensional Response Curve for the Duffing Oscillator

Exact analytical solutions of Duffing's equation (4) do not exist and therefore approximation schemes are used in quantitative investigations. One of the approximation methods that has been widely adopted is the harmonic balance method. This involves re-arranging the external excitation in (4) as

$$u = P \sin(\omega t) + Q \cos(\omega t) \quad \text{with } A = \sqrt{P^2 + Q^2} \quad (5)$$

and expressing the response as

$$y = H \sin(\omega t) \quad (6)$$

Substituting (5) and (6) into (4), together with the use of  $\sin^3(t) = \frac{3}{4}\sin(t) - \frac{1}{4}\sin(3t)$  yields

$$\frac{3}{4}k_3H^3 \sin(\omega t) - mH\omega^2 \sin(\omega t) + cH \sin(\omega t) + k_1H\omega \cos(t) = P \sin(t) + Q \cos(t) \quad (7)$$

where the term containing  $\sin(3\omega t)$  has been neglected.

Equating coefficients of the same harmonic terms in (7) and using  $A = \sqrt{P^2 + Q^2}$  gives

$$\left[\frac{3}{4}k_3H^3 + (k_1 - m\omega^2)H\right]^2 + c^2\omega^2H^2 = A^2 \quad (8)$$

If the amplitude  $A$  and frequency  $\omega$  of the excitation are given, the amplitude of the response can be approximately obtained using formula (8). One important phenomenon which commonly occurs with the Duffing oscillator is the so-called hysteresis or jump phenomenon which occurs because of the multi-valued properties of the response in (8) due to the cubic nonlinearity. This will be shown as two stable solutions separated by an unstable solution.

Hysteresis can occur by either changing the amplitude or the frequency of the external excitation and has been studied extensively based on the response curve(RC), which



measures the amplitude of the response against either the amplitude or the frequency of excitation in a 2-dimensional diagram. Whereas hysteresis occurs along both the amplitude and frequency axes, it is sometimes advantageous to have a 3-dimensional response curve which can provide a global picture of the hysteresis behaviour. Here a 3-dimensional response curve of the Duffing oscillator (4) is shown in Figure 1, using the parameters  $m = 1, c = 0.2, k_1 = 1$  and  $k_3 = 0.05$ . Note that only forward paths where the frequency and amplitude are increasing are studied.

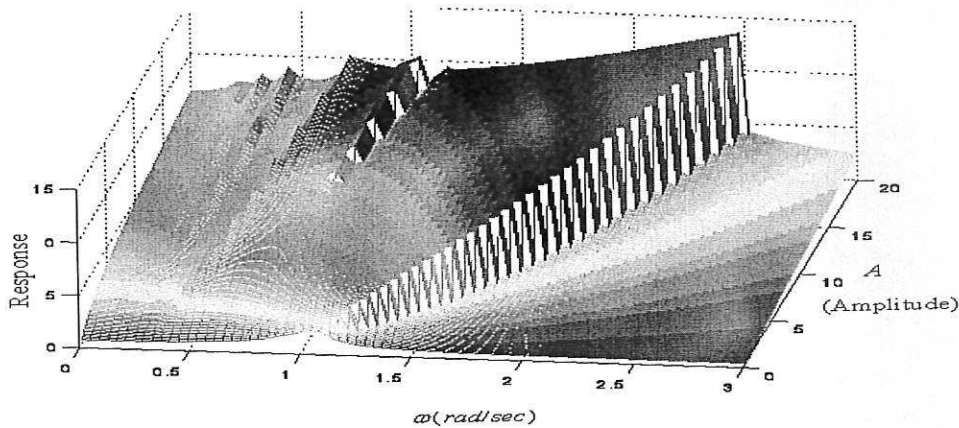


Figure 1. Response curve of the Duffing oscillator (4) for both varying excitation amplitude and frequency

Figure 1 reveals a lot of important information with respect to hysteresis. It gives a clear overall picture of when and where the jump occurs. Overall, there are two areas where hysteresis is present. The major jump cliff starting from  $\omega = 1 \text{ rad/sec}$  and  $A=1$  has been the main subject of most studies. Looking along the frequency axis, it can be seen that there is only a very narrow range of excitation amplitudes where the Duffing system is hysteresis-free, for example where  $A \in [0, 0.5]$ . The main jump cliff starts from  $A=0.5$ . The frequency point and the magnitude of the jump increases monotonously, as the amplitude of the excitation increases. When the amplitude reaches around 10.5, multiple jumps appear.

Along the amplitude axis, over the low frequency range, there is an area where no hysteresis is present. But there are ridges as the amplitude becomes high, indicating an increase of dynamic complexity due to the increasing excitation amplitude. There are also no multiple jumps for the whole frequency range. In the following section, a frequency domain analysis is performed on both axes to further characterize this type of severe nonlinearity.

#### 4. Frequency Domain Analysis of Hysteresis

Although the 3-D Response Curve illustrated in Figure 1 provides a comprehensive picture with respect to the hysteresis, the features it reveals are mostly in the time domain. Very few efforts have been made to analyse the dynamics of hysteresis in the frequency domain. In this section, an attempt has been made for the first time, by

combining the powerful Response Spectrum Map recently proposed by Billings and Boaghe (2001), to exploit the frequency domain properties behind hysteresis at representative amplitude and frequency points.

#### 4.1 Frequency domain analysis for the Duffing equation when the amplitude of Excitation is held constant

From Figure 1, it can be seen that when the amplitude  $A$  is relatively small, there is only a single jump along the whole frequency axis. A 2-dimensional response curve can be extracted from Figure 1 by setting  $A=1.2$ , this is shown in Figure 2.

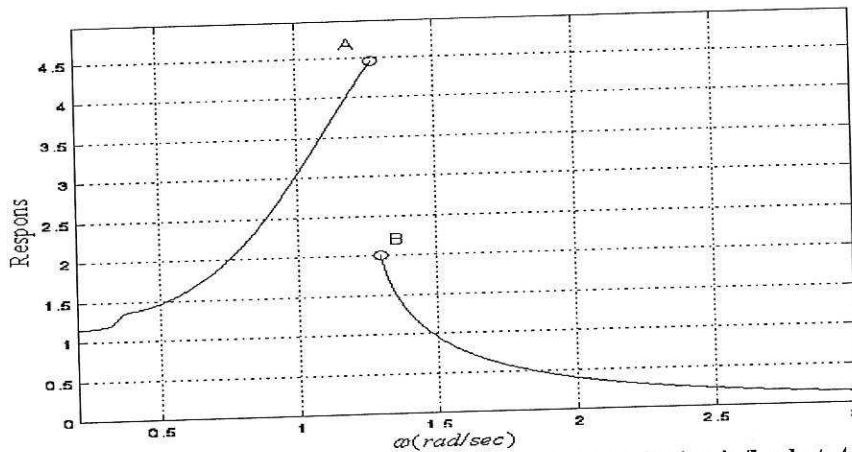


Figure 2. 2D Response curve when the amplitude of the excitation is fixed at  $A=1.2$

Apart from the fact that the hysteresis occurs at  $\omega = 1.28 \text{ rad/sec}$  point, Figure 2 shows very little other information about the properties of the system before and after the jump. A completely new 3-D diagram, called the Response Spectrum Map (RSM) by Billings and Boaghe (2001) which is typically used to study bifurcation phenomena, will be adopted here in the analysis of hysteresis. The RSM for the Duffing oscillator (4) at amplitude  $A=1.2$  is illustrated in Figure 3. It can be seen from Figure 3 that a significant frequency component change occurs in the response at excitation frequency  $\omega = 1.28 \text{ rad/sec}$  in line with the response curve in Figure 2. But the important information the response curve cannot provide but the RSM can is that over the whole excitation frequency range, the response possesses only first, third and fifth order etc harmonics, implying that the underlying Duffing oscillator at amplitude  $A=1.2$  is weakly nonlinear, or in other words, has a Volterra series representation. Although no global Volterra expression is available because the two stable solutions co-exist, local Volterra series representations can be realised.

$|H_1(\cdot)|$  compared with the result at  $\omega = 1.29$ , suggesting that in the latter case the system can be almost approximated by a linear system.

	$\omega = 1.28$	$\omega = 1.29$
$ H_1(\omega) $	3.7552	1.8310
$ H_3(\omega, \omega, \omega) $	0.1973	0.0222
$ H_3(\omega, \omega, -\omega) $	0.1952	0.0163

**Table 1. Comparison of the GFRF's from (9) and (10)**

The contribution of each GFRF's can also be calculated using the results in Bedrosian and Rice(1971). Figure 4 and 5 illustrate the contributions from each order of GFRF's to the response at points A and B respectively using NX models (9) and (10). It can be seen in Figure 4 that both the first and third order GFRF are required to obtain a satisfactory truncation accuracy at  $\omega=1.28$ , while in Figure 5 for  $\omega=1.29$  there is no apparent improvement in the accuracy when the third order GFRF is included. In other words, at  $\omega=1.29$  the system can be almost regarded as a linear system. These findings are in good agreement with the observation from the RSM in Figure 3. It can therefore be concluded that there is a reduction in the number of terms in the Volterra representation after the hysteresis effects.

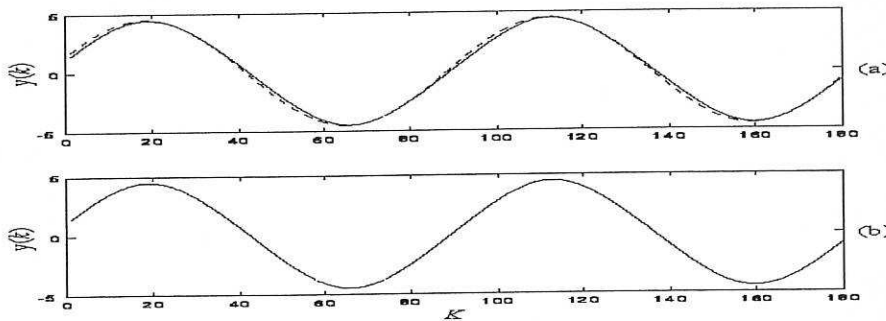


Figure 4 (a) First order output response, and (b) up to the third order output response. Dashed—synthesized output by GFRF's from (9); Solid—simulated original output from (4)

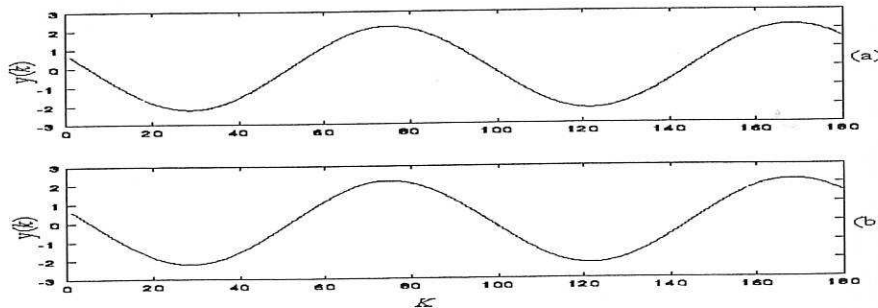


Figure 5 (a) First order output response, and (b) up to the third order output response. Dashed—synthesized output by GFRF's from (10); Solid—simulated original output from (4)



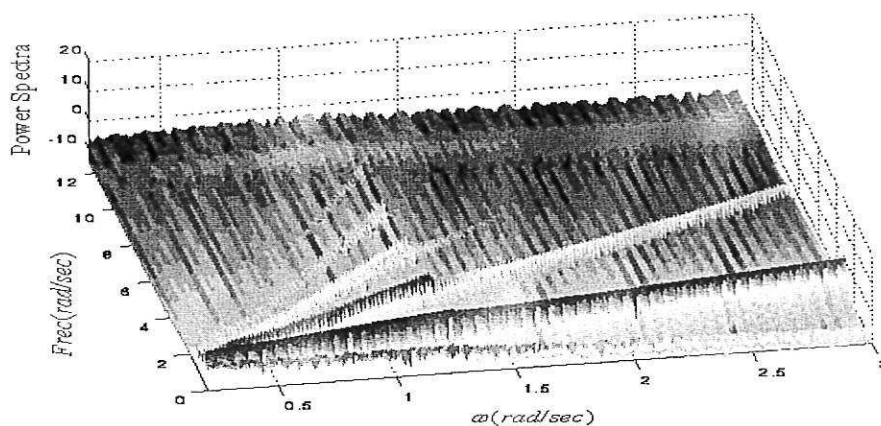


Figure 3. Response Spectrum Map for the case where the amplitude of excitation is fixed at  $A=1.2$

Further analysis of the RSM in Figure 3 reveals that although the system preserves the Volterra series validity throughout the hysteresis dynamics, the level of changes with various harmonics are different. It can be seen that the first order harmonic remains relatively unchanged before and after the hysteresis effect, while a significant drop in magnitude occurs for the higher order frequency components after hysteresis, with the fifth harmonics even vanishing. Since the higher order harmonics are related to the higher order kernels in the Volterra series representation, this phenomenon would suggest a reduced order Volterra representation after the hysteresis. To verify this, two discrete time Volterra (NX) models were built using the excitation and response data at points A and B in Figure 2 respectively. That is for the points just before ( $\omega=1.28$ ) and after ( $\omega=1.29$ ) the jump. The models were estimated using the orthogonal least squares algorithm with terms selection based on the error reduction ratio (Billings *et al* 1988).

Model for point A ( $\omega=1.28$ ):

$$y(k) = 46.117 u(k-4) - 43.877 u(k-3) - 0.12283 u(k-1)u(k-2)u(k-4) - 0.07454 u(k-1)u(k-2)u(k-3) \quad (9)$$

Model for point B ( $\omega=1.29$ ):

$$y(k) = -6.212 u(k-1) + 4.7472 u(k-4) + 0.25188 u^3(k-4) - 0.23702 u(k-3)u^2(k-4) \quad (10)$$

Inspection of the coefficients of the NX model (9) and (10) does not readily reveal which model has a more significant higher order (third order) presence in terms of a Volterra representation. But if both (9) and (10) are mapped into the frequency domain (Peyton Jones and Billings, 1989) and the Generalised Frequency Response Functions (GFRF's) are compared (Table 1), the order of Volterra representation or the mildness of nonlinearity for each situation becomes very clear. It can be seen from Table 1 that the magnitude of the higher order GFRF's  $|H_3(\cdot)|$  with  $\omega=1.28$  is much more significant than the first order

It can be seen from the 3-D response curve in Figure 1 that the complexity of the dynamics increases as the amplitude of the excitation increases, leading to multiple jumps. Figure 6 shows the response curve at amplitude  $A=15$ . It can be seen from Figure 6 that at  $A=15$  there are much richer dynamic behaviours compared to the response curve at amplitude  $A=1.2$  in Figure 2. There are more resonances in the low frequency range, and in addition to the main jump at around  $\omega=2.3$ , there is an auxiliary jump at around  $\omega=0.96$ .

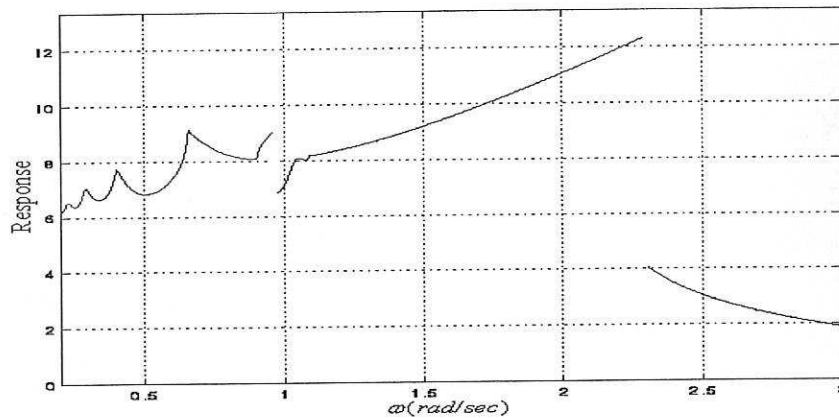


Figure 6. Response curve when the amplitude of excitation is fixed at  $A=15$

The RSM for the Duffing equation (4) at  $A=15$  is given in Figure 7. The phenomenon surrounding the main jump at around  $\omega=2.3$  is similar to that for  $A=1.2$ , with a possible reduced Volterra representation after the jump. The particular feature of the RSM in Figure 7 compared with the RSM in Figure 3 is the presence of hysteresis at  $\omega=0.96$ , apparently initiated by the existence of even order harmonics, which can not be interpreted in the frequency domain from the original structure of the Duffing oscillator where there is no quadratic nonlinearity.

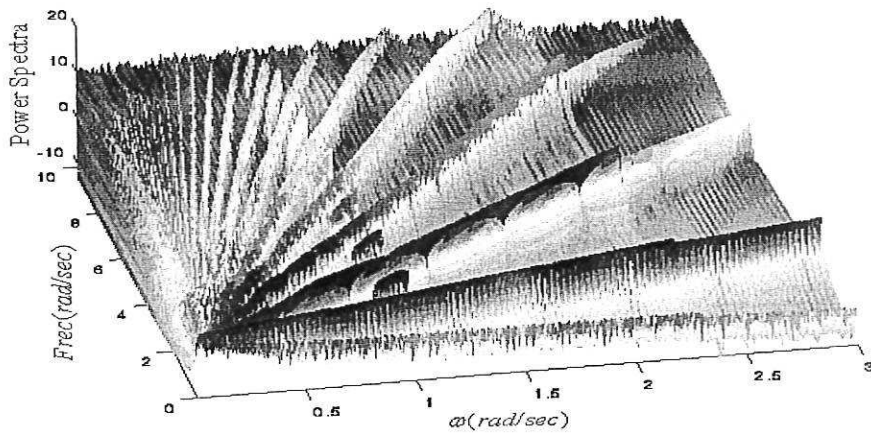


Figure 7. Response Spectrum Map for the amplitude of excitation fixed at  $A=15$

#### 4.2 Frequency domain analysis for Duffing equation when the frequency of excitation is held constant

Hysteresis can occur along the amplitude axis as well as the frequency axis, as the 3-dimensional response curve in Figure 1 revealed. The response spectrum map can also play an important role in the qualitative analysis in this situation.

First, the excitation frequency is chosen as  $\omega=1.52$  rad/sec. The corresponding response curve and RSM are shown in Figure 8 and 9 respectively. It can be seen from the RSM in Figure 9 that there is a dominant presence of first harmonics in the response both before and after hysteresis. This confirms the implication of the harmonic balance solution in equation (8) that the solution is dominated by the first order harmonic. Therefore the two monotonously increasing curves in Figure 6 can be considered as reflecting the two stable solution orbits in equation (8) separated by the unstable solution.

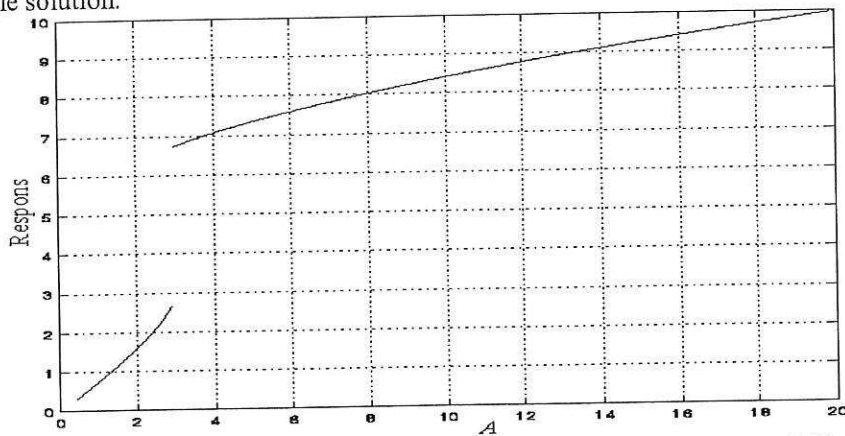


Figure 8. Response curve for the frequency of excitation fixed at  $\omega=1.52$

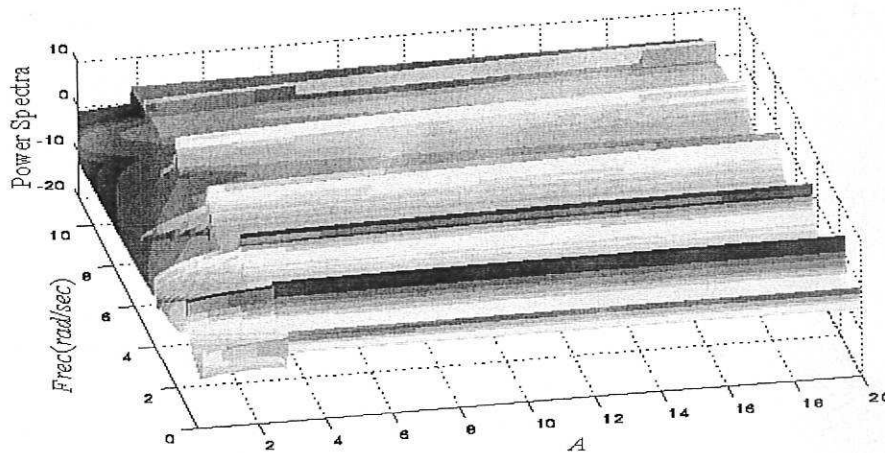


Figure 9. Response spectrum map for the frequency of excitation fixed at  $\omega=1.52$

From Figure 9 it can be seen that throughout the whole amplitude range, there are only first order and associated odd order superharmonics, similar to the constant amplitude case in Figure 3, indicating that local Volterra series representations exist. Again, the significant higher order harmonics suggest that the order of Volterra representation increases after the jump.

Now consider the situation when the frequency of the excitation is held constant at  $\omega=1$ . The response curve and the response spectrum map are shown in Figures 10 and 11 respectively.

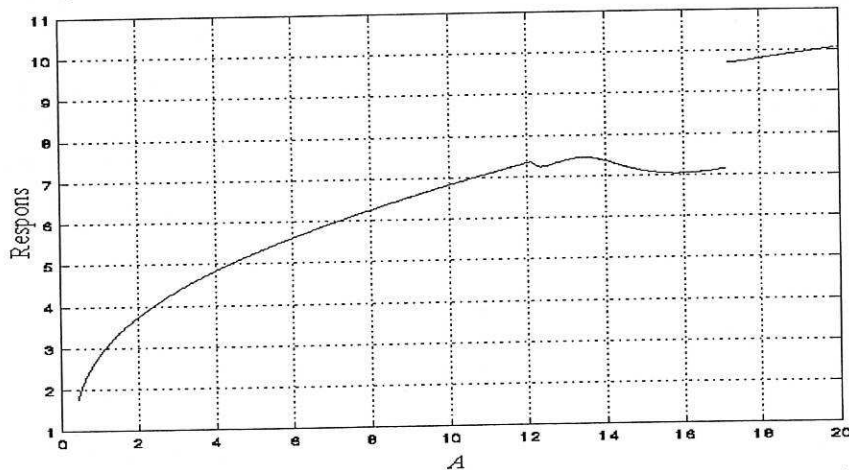


Figure 10. Response curve for the frequency of excitation fixed at  $\omega=1$

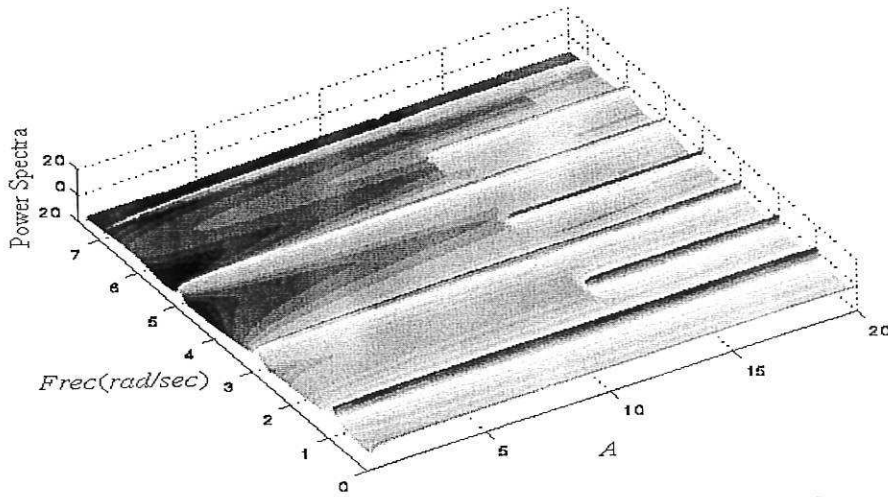


Figure 11. Response spectrum map for the frequency of excitation fixed at  $\omega=1$

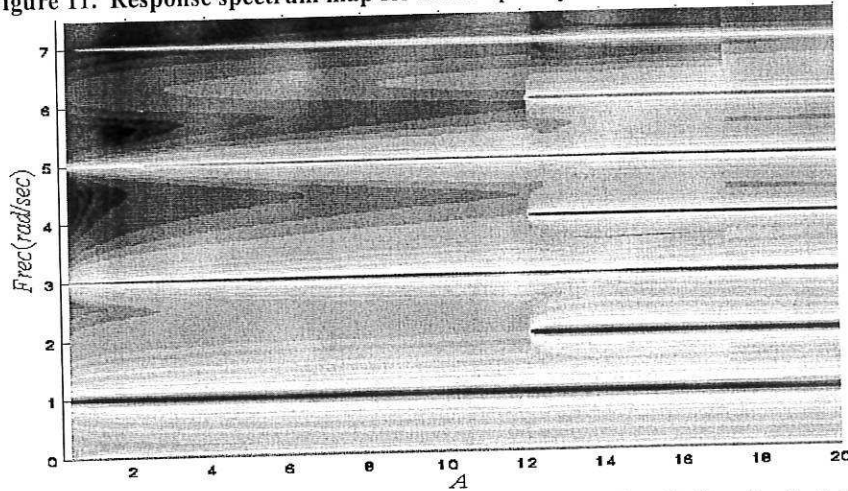


Figure 12. 2D Response spectrum map for the frequency of excitation fixed at  $\omega=1$

The parameter  $k_3$  in the Duffing oscillator model (4) was chosen to be small to give a weak nonlinearity under some conditions, as shown in the previous analysis. However, the validity of the Volterra series also depends externally on the amplitude of the excitation. As the amplitude of excitation increases, the dynamics of the Duffing oscillator change accordingly, and the system may become severely nonlinear and no valid local Volterra representation will exist. By studying the response in both the time and the frequency domains using the response curve and the response spectrum map with respect to the excitation amplitude, the influence of the amplitude on the nonlinear dynamics becomes much clearer.

From Figure 11 it can be seen that for the lower amplitude range  $A < 12.2$ , there are standard first and odd higher order harmonics in the response, suggesting a weak nonlinearity for this region. For  $A > 12.2$ , strong second order harmonics are present, together with even order super-harmonics, resulting in the significant behaviour change shown in Figure 10. The presence of even order harmonics leads to further weak occurrences of harmonics at 4.5 rad/sec and 5.5 rad/sec etc. These are more visible in Figure 12 which is the 2-dimensional overhead view of Figure 11, at



$A=17.4$ , which seemly initiates the hysteresis. This is a region that cannot be represented by a local Volterra series model. Unlike previous cases where there are very apparent changes in the harmonics in the response when the hysteresis is initiated, in this case no obvious major harmonic changes occur. Therefore this might be an interesting example where very small frequency domain changes result in significant changes in the time domain behaviour.

## 5. Conclusions

Hysteresis, which is caused by multi-valued solutions, belongs to the class of severe nonlinear phenomena and commonly appears in the Duffing oscillator. Hysteresis can be initiated by either varying the amplitude or the frequency of excitation. Traditionally 2-dimensional response curves have been used for the analysis of this important nonlinear phenomenon. In this study a 3-dimensional response curve has been generated to provide a comprehensive analysis of hysteresis for variations in both the amplitude and the frequency of excitation. The 3-dimensional response curve clearly shows that hysteresis is a combined effect of excitation frequency and amplitude, resulting in a seemly continuous cliff-effect map.

Although the response curves are useful in identifying the operating values associated with initiating hysteresis in the Duffing oscillator and in assessing the magnitude of the jumps, they mainly provide time domain information. It is well known that though hysteresis cannot be modelled by a global Volterra series due to the multiple steady state solutions, there are local Volterra series representations which exist in some situations when the amplitude of excitation is relatively small. In these operating conditions, a frequency domain Volterra series analysis can be performed using the GFRF's. It is therefore desirable to have a supplementary frequency domain tool to help to identify the characteristics of the nonlinearity. This has been achieved in this study by the introductory of the response spectrum map. It has been shown that the response spectrum map can provide a quick assessment of the validity of the Volterra series representation, the mildness of the nonlinearity, the truncation order of the Volterra series, and which harmonics play a part in the dynamic changes. The frequency domain information thus provides more clues and a better understanding of the mechanisms behind hysteresis.

**Acknowledgement:** The authors gratefully acknowledge that this work was supported by the Engineering and Physical Sciences Research Council(EPSRC) UK.

### References:

- Bedrosian, E. and Rice, S. O., 1971, "The output properties of Volterra systems (nonlinear systems with memory) driven by harmonic and Gaussian inputs," *Proc. IEEE*, Vol 59, pp.1688-1707.



- Billings, S.A. and Boaghe, O.M., 2001, The response spectrum map, a frequency domain equivalent to the bifurcation diagram, *Int. J. of Bifurcation and Chaos*, Vol.11, No.7, pp.1961-1975.
- Billings, S.A., Korenberg, M.J., and Chen, S., 1988, Identification of non-linear output-affine systems using an orthogonal least-squares algorithm, *Int. J. Systems Science*, Vol. 19, pp. 1559-1568.
- Hagedorn, P., 1982, *Non-linear oscillations*, Clarendon Press, Oxford.
- Peyton Jones, J.C. and Billings, S.A., 1989, A Recursive algorithm for computing the frequency response of a class of non-linear difference equation models, *Int.J.Control*, Vol.50, No.5, pp.1925-1940.
- Stoker, J.J., 1950, *Nonlinear vibrations in Mechanical and Electrical Systems*, Interscience Publishers Inc, New York.
- Thompson, J. M. T. and Stewart, H. B., 2002, *Nonlinear Dynamics and Chaos*, John Wiley & Sons Ltd, England.
- Volterra, V., 1930, *Theory of Functionals*, Blackie and Sons.